Zeolite Married to Carbon: A New Family of Membrane Materials with Excellent Gas Separation Performance

Qingling Liu,[†] Tonghua Wang,*[,†] Changhai Liang,[†] Bing Zhang,[†] Shili Liu,[†] Yiming Cao,[‡] and Jieshan Qiu*[,†]

Carbon Research Laboratory, Center for Nano Materials and Science, State Key Laboratory of Fine Chemicals, School of Chemical Engineering, Dalian University of Technology, 158 Zhongshan Road, P.O. Box 49, Dalian 116012, China, and Key Laboratory for Micro/Nano Technology and System of Liaoning Province, Dalian University of Technology, Dalian 116023, China, and Dalian Institute of Chemical Physics, Chinese Academy of Sciences, Dalian 116023, China

Received August 1, 2006. Revised Manuscript Received September 30, 2006

Novel carbon/zeolite nanocomposite membranes with tailorable gas transport properties were fabricated by pyrolysis of polyamic acid/zeolite nanocomposites. The microstructure and gas permeability of these chemically robust materials were altered by varying zeolite loading and final pyrolysis temperature. Characterization of the as-synthesized composite membranes by SEM, XRD, and TEM revealed that the zeolite particles adhered well to the carbon matrix and that the microstructure of the zeolite was not destroyed during pyrolysis. Gas permeation tests using small molecules (H_2, CO_2, O_2, N_2) indicated that the composite membranes exhibited outstanding permeability together with high selectivity and followed the molecular sieve mechanism. It is believed that the zeolite embedded in the carbon matrix decreased the gas diffusion resistance and improved the gas permeation rate. The excellent gas transport properties for all test gases make the carbon/zeolite composite an attractive membrane material in gas separation areas.

Introduction

Membrane-based separation is attractive for molecular-scale separations because of its low energy requirements and excellent reliability.[1] In particular, in the gas separation market, the membrane technology is a quite young and eye-opening technology. In past decades, polymeric membranes have been commercially used for gas separation, for example, in hydrogen recovery, oxygen, or nitrogen enrichment, olefin/paraffin separation, natural gas dehydration, and acid gas treatment. However, polymeric membranes for gas separations have been known to have a tradeoff between permeability and selectivity as shown in the upper bound curves developed by Robeson.[2] It appears that, to exceed this limit, new materials need to be developed. In recent years, inorganic membranes such as micro- and mesoporous silica membranes,[3] zeolite membranes,[4] nanoporous carbon membranes,[5] and carbon/silica membranes[6] were quickly developed, and they offer outstanding potential for application in gas separation. These membranes can separate specific gas molecules more effectively by molecular recognition at the subnanometer level on the basis of a "molecular sieving mechanism". In particular, zeolite membranes and carbon membranes have been targeted for potential applications as gas molecular separation membranes, because of their true molecular selectivity for gas mixtures with similar molecular size, good durability, excellent mechanical strength under high pressure, and superior chemical and thermal stability. To date, numerous types of zeolite membranes and carbon membranes have been developed in various forms such as supported zeolite (carbon) membranes,[1,7] flat sheet homo-

* Corresponding authors. E-mail: wangth@chem.dlut.edu.cn; jqiu@dlut.edu.cn.
[†] Dalian University of Technology.
[‡] Chinese Academy of Sciences.

(1) (a) Lin, H.; Wagner, E. V.; Freeman, B. D.; Toy, L. G.; Gupta, R. P. *Science* **2006**, *311*, 639. (b) Shiflett, M. B.; Foley, H. C. *Science* **1999**, *285*, 1902. (c) Lai, Z.; Bonilla, G.; Diaz, I.; Nery, J. G.; Sujaoti, K.; Amat, M. A.; Kokkoli, E.; Terasaki, O.; Thompson, R. W.; Tsapatsis, M.; Vlachos, D. G. *Science* **2003**, *300*, 456. (d) Merkel, T. C.; Freeman, B. D.; Spontak, R. J.; He, Z.; Pinnau, I.; Meakin, P.; Hill, A. J. *Science* **2002**, *296*, 519.

(2) Robeson, L. M. *J. Membr. Sci.* **1991**, *62*, 165.

(3) (a) De Vos, R. M.; Verweij, H. *Science* **1998**, *279*, 1710. (b) Lu, Y.; Ganguli, R.; Drewien, C. A.; Anderson, M. T.; Brinker, C. J.; Gong, W.; Guo, Y.; Soyez, H.; Dunn, B.; Huang, M. H.; Zink, J. I. *Nature* **1997**, *389*, 364.

(4) (a) Yuan, W.; Lin, Y. S.; Yang, W. *J. Am. Chem. Soc.* **2004**, *126*, 4776. (b) Zhang, F.; Fuji, M.; Takahashi, M. *Chem. Mater.* **2005**, *17*, 1167. (c) Giannakopoulos, I. G.; Nikolakis, V. *Ind. Eng. Chem. Res.* **2005**, *44*, 226.

(5) (a) Shiflett, M. B.; Pedrick, J. F.; Mclean, S. R.; Subramoney, S.; Foley, H. C. *Adv. Mater.* **2000**, *12*, 21. (b) Fuertes, A. B. *J. Membr. Sci.* **2000**, *177*, 9. (c) Liang, C.; Sha, G.; Guo, S. *Carbon* **1999**, *37*, 1391. (d) Steel, K. M.; Koros, W. J. *Carbon* **2005**, *43*, 1843. (e) Suda, H.; Haraya, K. *J. Phys. Chem. B* **1997**, *101*, 3988. (f) Hayashi, J.; Mizuta, H.; Yamamoto, Y.; Kusakabe, Y. K.; Morooka, S. *J. Membr. Sci.* **1997**, *124*, 243. (g) Tin, P. S.; Chung, T. S.; Kawi, S.; Guiver, M. D. *Microporous Mesoporous Mater.* **2004**, *73*, 151. (h) Tin, P. S.; Chung, T. S.; Hill, A. J. *Ind. Eng. Chem. Res.* **2004**, *43*, 6476. (i) Lu, S.; Chung, T. S.; Wensley, G. S. H.; Pramoda, K. P. *J. Membr. Sci.* **2004**, *244*, 77. (j) Lu, S.; Chung, T. S.; Pramoda, K. P. *Microporous Mesoporous Mater.* **2005**, *84*, 59.

(6) (a) Park, H. B.; Lee, Y. M. *Adv. Mater.* **2005**, *17*, 477. (b) Park, H. B.; Suh, I. Y.; Lee, Y. M. *Chem. Mater.* **2002**, *14*, 3034. (c) Park, H. B.; Lee, Y. M. *J. Membr. Sci.* **2003**, *213*, 263. (d) Park, H. B.; Jung, C. H.; Kim, Y. K.; Lee, S. Y.; Nam, S. Y.; Lee, Y. M. *J. Membr. Sci.* **2004**, *235*, 87.

(7) (a) Lai, Z.; Tsapatsis, M.; Nicolich, J. P. *Adv. Funct. Mater.* **2004**, *14*, 716. (b) Wang, Z.; Yan, Y. *Chem. Mater.* **2001**, *13*, 1101. (c) Li, S.; Li, Z.; Bozhilov, K. N.; Chen, Z.; Yan, Y. *J. Am. Chem. Soc.* **2004**, *126*, 10732. (d) Seike, T.; Matsuda, M.; Miyake, M. *J. Am. Ceram. Soc.* **2004**, *87*, 1585.

10.1021/cm061807e CCC: $33.50 © 2006 American Chemical Society
Published on Web 11/30/2006

geneous pyrolytic carbon membranes,[5e,8] and hollow fiber carbon membranes[9] by varying the fabrication methods. However, for zeolite membranes, it is difficult to control the thickness, grain size, and orientation of the membrane during the fabrication progress.[10] Carbon membranes are generally fabricated by pyrolysis of polymer materials, and compared to zeolite membranes, their thickness and morphology are easily controlled by varying the polymer properties, but it remains a challenge to fabricate microporous products with high permeability and excellent selectivity.

The concepts for the rational design of novel materials with superior characteristics and properties have been previously demonstrated in the fields of science and engineering of supramolecular polymers,[11] polymer nanocomposites,[12] and catalysts.[13] Common fabrication processes to produce these tailor-made nanomaterials are based on a physical/chemical fundamental that recognizes how materials are assembled starting from the atomic scale, to the nanoscale, and ending at the bulk scale.[14] One of these processes involves the incorporation of a second organic or inorganic nanophase into the polymeric materials. This technique was successful in the production of novel membrane materials.[15] In a previous study, we reported the controlled fabrication of carbon/ZSM-5 nanocomposite membranes through the pyrolysis of polyimide (PI)/ZSM-5 precursors.[16] That study indicated that the permeability of the composite membrane could be improved by incorporating nano-ZSM-5 into the carbon membranes. The motivation for us to incorporate zeolite as filler into the carbon matrix is because ZSM-5 is a thermally stable material and could provide transport pathways for gas molecules (Figure 1). In the present study, we report series membrane materials with excellent permeability and selectivity designed by tuning the pyrolysis conditions and varying the zeolite loading.

Experimental Section

Starting Materials. Polyamic acid (PAA) derived from pyromellitic dianhydride and 4,4-oxydianiline were obtained from Tianjin Tianyuan Electronic Material Co., Ltd. (Tianjin, China) and used without further purification. The nanosized ZSM-5 (20−50 nm, Si/Al ratio: 12.5) used was synthesized according to the method reported by Van Grieken et al.[17] *N*,*N*-Dimethylacetamide (DMAc) was obtained from Tianjin Kermel Chemical Reagent Co., Ltd. (Tianjin, China) and was distilled by a revolving alembic.

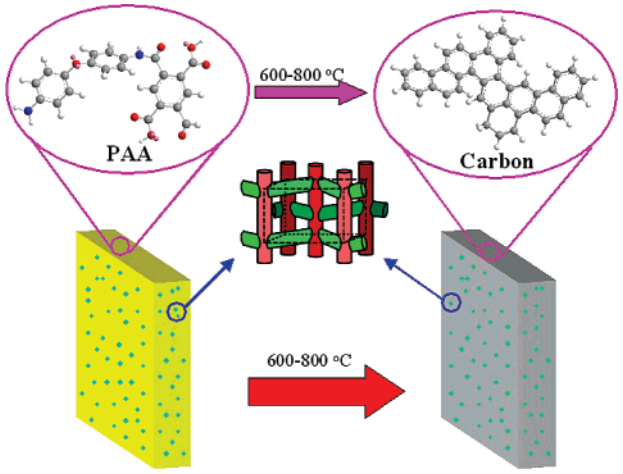

Figure 1. Proposed model for the carbon/zeolite composite membranes.

Table 1. Sample Designations and Compositions of the Precursors

sample	ZSM-5 (g)	PAA (g)	wt % (ZSM-5)
PIZ1	0.3	20	4.76
PIZ2	0.6	20	9.09
PIZ3	1.2	20	16.7

Preparation of Precursors. The chemical compositions of the precursors used in this study are summarized in Table 1. The zeolite ZSM-5 powder was dispersed in DMAc under stirring and ultrasonic treatment for 2 h, and then the mixture was added dropwise to a PAA solution (30 wt %). After the mixture was stirred for 10 h at room temperature, a homogeneous yellowish PAA-containing zeolite solution was obtained. The resulting homogeneous solution was cast on a glass plate and then dried at 40 °C for 12 h. These PAA/zeolite composite membranes were stored until use in a desiccator containing dry silica gel to avoid humidity.

Preparation of Carbon/Zeolite Composite Membranes. The pyrolysis conditions, such as the final pyrolysis temperature, heating rate, and pyrolysis atmosphere, are the most important factors determining the microstructure and gas permeation properties of the composite membranes. The carbon/zeolite composite membranes obtained in this work were prepared by the pyrolysis of PAA/zeolite precursors with different compositions. Before each pyrolysis trial, the freestanding PAA/zeolite precursors were cut into small pieces with a diameter of 46 mm and were put between graphite plates supported by a metal shelf. Then, the PAA/zeolite membranes were pyrolyzed under Ar atmosphere in a metal tube furnace equipped with a programmed temperature controller. The Ar flow was precisely controlled at 100 cm^3 (STP)/min by a mass flow controller.

An important objective of this work was to study the changes in gas permeability of the composite membrane as it progresses from low temperature to high temperature. To study this progress, pyrolysis was ended at three different final temperatures (600, 700, and 800 °C). Figure 2 shows the temperature−time protocol used for the pyrolysis of the precursors.

In the initial stage, the heating rate was 3−5 °C/min from room temperature to 350 °C. During this process, PAA was thermally imidized, which helps to produce strong and flexible PI/zeolite membranes. The heating rate was decreased to 2 °C/min until the temperature reached 600, 700, and 800 °C. Then, the composite

(8) Singh-Ghosal, A.; Koros, W. J. *J. Membr. Sci.* **2000**, *174*, 177.
(9) (a) Geiszler, V. C.; Koros, W. J. *Ind. Eng. Chem. Res.* **1996**, *35*, 2999. (b) Vu, D. Q.; Koros, W. J. *Ind Eng. Chem. Res.* **2002**, *41*, 367. (c) David, L. I. B.; Ismail, A. F. *J. Membr. Sci.* **2003**, *213*, 285.
(10) (a) Hedlund, J.; Sterte, J.; Anthonis, M.; Bons, A. J.; Carstensen, B.; Corcoran, N.; Cox, D.; Deckman, H.; Gijnst, W. D.; Moor, P. P.; Lai, F.; Henry, J. M.; Mortier, W.; Reinoso, J.; Peters, J. *Microporous Mesoporous Mater.* **2002**, *52*, 179. (b) Gouzinis, A.; Tsapatsis, M. *Chem. Mater.* **1998**, *10*, 2497.
(11) Schubert, U. S.; Eschbaumer, C. *Angew. Chem., Int. Ed.* **2002**, *41*, 2892.
(12) *Polymer Nanocomposites: Synthesis, Characterization, and Modeling*; Krishnamoorti, R., Vaia, R. A., Eds.; ACS Symposium Series 804; American Chemical Society: Washington, DC, 2002.
(13) Tanev, P. T.; Chibwe, M.; Pinnavaia, T. J. *Nature* **1994**, *368*, 321.
(14) Balzani, V.; Credi, A.; Raymo, F. M.; Stoddart, J. F. *Angew. Chem., Int. Ed.* **2000**, *39*, 3348.
(15) (a) Koros, W. J.; Mahajan, R. *J. Membr. Sci.* **2000**, *175*, 181. (b) Vu, D. Q.; Koros, W. J.; Miller, S. J. *J. Membr. Sci.* **2003**, *211*, 311. (c) Wang, H. T.; Holmberg, B. A.; Yan, Y. S. *J. Mater. Chem.* **2002**, *12*, 3640. (d) Wang, H. T.; Huang, L. M.; Holmberg, B. A.; Yan, Y. S. *Chem. Commun.* **2002**, *16*, 1708.
(16) Liu, Q. L.; Wang, T. H.; Qiu, J. S.; Cao, Y. M. *Chem. Commun.* **2006**, 1230.
(17) Van Grieken, R.; Sotelo, J. L.; Menendez, J. M.; Melero, J. A. *Microporous Mesoporous Mater.* **2000**, *39*, 135.

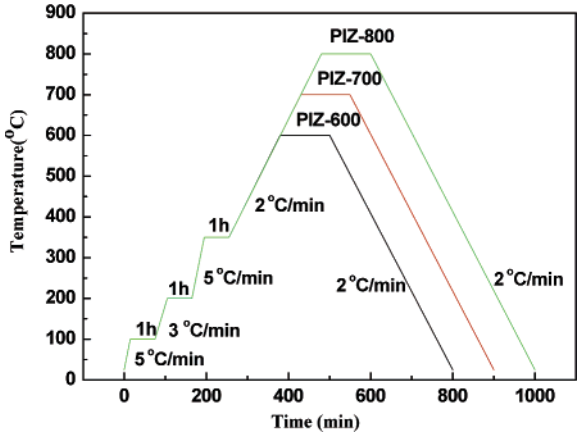

Figure 2. Temperature/time protocols for pyrolysis of precursors.

membranes were kept at 600 °C (denoted PIZ-600), 700 °C (denoted PIZ-700), and 800 °C (denoted PIZ-800) for 2 h. Finally, the furnace was cooled to room temperature at 2 °C/min. The obtained carbon/zeolite composite membranes (around 55 ± 5 μm thick, measured by a electronic digital micrometer) were taken from the furnace and then stored in desiccators containing dry silica gel to minimize the effects of humidity.

Characterization Methods. The surface and cross-sectional morphologies of the carbon/zeolite composite membranes were observed by a JEOL-5600LV scanning electron microscopy (SEM; JEOL, Inc., Kyoto, Japan) at 30 kV. Wide-angle X-ray diffraction was performed to qualitatively measure the structure of the zeolite and composite membranes on a diffractometer equipped with graphite-monochromatized Cu Kα radiation in the 2θ angle range from 5° to 60°. Transmission electron microscopy (TEM) images were taken on a JEOL JEM-2000EX microscope (JEOL, Inc.) with a ReB_6 filament and an accelerating voltage of 200 kV. Samples of the zeolite and composite membranes for examination were prepared via sonication of a powdered sample in ethanol for 10 min and evaporation of two drops of the suspension onto a holey carbon film supported on a 3-mm, 400 mesh copper grid.

Gas Permeation Performance. The gas permeation performance of the composite membranes was determined using the single gas permeation technique by the variable volume/constant pressure method.[18] The tested gases included H_2, CO_2, O_2, and N_2, and the purity of all the test gases was >99.99%. The permeability coefficient for a permeated gas is determined by multiplying the permeance by the membrane thickness and can be obtained by

$$P = \frac{R}{A \cdot \Delta P / l} \tag{1}$$

where P is the permeability represented in Barrer (1 Barrer = 10^{-10} cm^3 (STP)cm/cm^2 s cmHg); R is the flux of gas permeating the membrane; A and l are the effective membrane area and membrane thickness, respectively; and ΔP is the pressure difference between the feed side and the permeate side. The ideal separation factor (gas selectivity) for components A and B is defined as the ratio of permeability of each component as

$$\alpha_{A/B} = \frac{P_A}{P_B} \tag{2}$$

In this study, the effective area of the membranes was 6 cm^2, and the operating temperature was 25 °C. For each membrane, measurements were conducted more than three times, and the reported final results are the averaged ones. The precision in the permeability measurements is estimated to be within 10%.

(18) Stern, S. A.; Gareis, P. J.; Sinclair, T. F.; Mohr, P. H. *J. Appl. Polym. Sci.* **1963**, *7*, 2035.

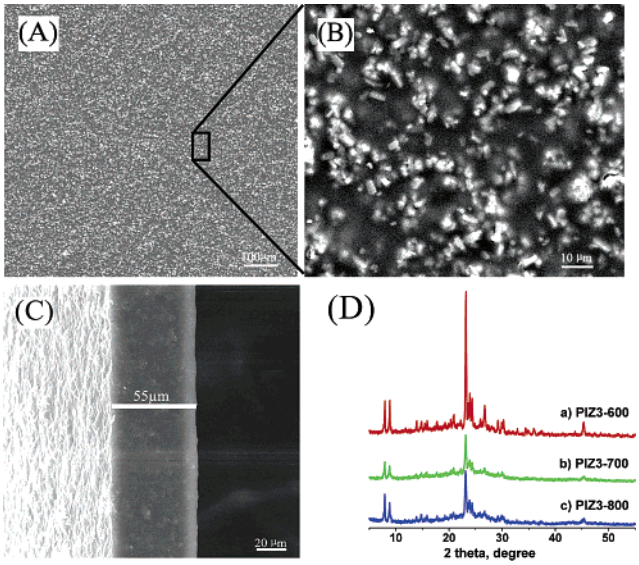

Figure 3. SEM images of the top surface (A), (B), and cross section (C) of the PIZ3-700 sample, and XRD patterns (D) of the PIZ3-600 (a), PIZ3-700 (b), and PIZ3-800 (c) samples.

Results and Discussion

Morphology and Structure of Carbon/Zeolite Composite Membranes. SEM images (Figure 3) show the top surface and cross-sectional morphology of the carbon/zeolite composite membranes. White spots indicate the zeolite (ZSM-5) crystals, and the black spots indicate the carbon domains. The zeolite crystals are well-dispersed in carbon matrix, and the membrane has a very smooth surface (Figure 3A). At high magnification (Figure 3B), no voids and defects between the zeolite crystal and the carbon phase are observed, suggesting good zeolite/carbon contact. The thickness of the composite membranes is about 55 μm (Figure 3C), which agrees with the result of the electronic digital micrometer.

X-ray diffraction is a useful tool for studying the structure of the zeolite and carbon on a molecular level. For traditional pure carbon, membranes only show a broad weak (002) peak, which can be attributed to the turbostratic carbon structure with randomly oriented graphitic carbon layers.[16] However, in the case of the composite carbon membranes, peaks with zeolite (ZSM-5) character can be observed. As shown in Figure 3D, the X-ray diffraction patterns of the PIZ3-600, PIZ3-700, and PIZ3-800 show typical ZSM-5 structures, indicating that the structure of the zeolite is not destroyed during the heat treatment. The well-kept zeolite structure, embedded in the carbon matrix, is believed to be a key factor in affecting the gas separation performance of the composite membranes. Once the structure of the zeolite is destroyed, it cannot help the gas molecular diffusion and the function of the zeolite would be lost.

To obtain more detailed structural insight, samples PIZ3-700 and PIZ3-800 were investigated by TEM analysis. The TEM images of the composite membranes are composed of amorphous carbon and dispersed zeolite crystals (Figure 4a). For the carbon phase, the microstructure is turbostratic,

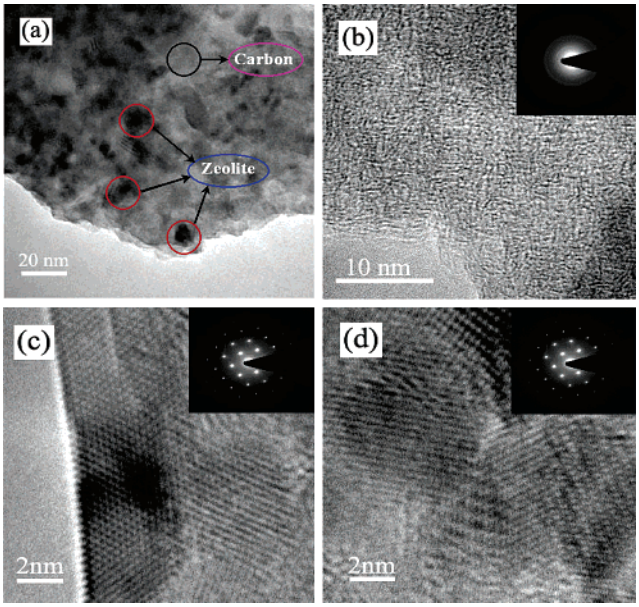

Figure 4. TEM images of composite membrane PIZ3-700 (a), carbon phase in the composite PIZ3-700 (b), and microstructure of the zeolite embedded in carbon (c) PIZ3-700 and (d) PIZ3-800.

composed of small microcrystalline carbon and amorphous carbon (Figure 4b).[19,20] The microchannels between the carbon layers can help to improve the gas selectivity. In Figure 4c,d, the crystal structure of zeolite ZSM-5 embedded in the carbon can be clearly observed. These images demonstrate that the crystal structure of the zeolite is not destroyed during pyrolysis, which agrees with the XRD results. The ordered channels in the zeolite provide pathways for the gas molecules to be separated.

Gas Permeation Properties of the Carbon/Zeolite Composite Membranes. To evaluate the gas permeability and selectivity of the carbon/zeolite composite membranes, single-component gas permeation tests were carried out through the as-obtained membranes using hydrogen (H_2, 2.89 Å), carbon dioxide (CO_2, 3.36 Å), oxygen (O_2, 3.46 Å), and nitrogen (N_2, 3.64 Å). It was found that the zeolite loading and the final pyrolysis temperature were two important factors in determining the microstructure and gas permeation properties of composite membranes.

Figures 5−7 illustrate the gas permeability at 25 °C for the carbon/zeolite composite membranes PIZ3, PIZ2, and PIZ3 prepared at different final pyrolysis temperatures (600, 700, and 800 °C). The gas permeability of the membranes is in the order PIZ3 > PIZ2 > PIZ1, which indicates that the permeability of the composite membranes is quite improved by increasing zeolite loading. It is well-known that zeolite ZSM-5 is a crystalline microporous material with an intricate channel system and uniform pores (∼5.5 Å). Thus, composite membranes with high zeolite loading possess more porosity. The continuous channels presented in the composites with the high zeolite loading allow the gas molecules to diffuse quickly through the zeolite and result in high gas permeation performance.

(19) Inagaki, M.; Ishida, T.; Yabe, K.; Hishiyama, Y. *Tanso* **1992**, 244.
(20) Hatori, H.; Yamada, Y.; Shiraishi, M.; Yoshihara, M.; Kimura, T. *Carbon* **1996**, *34*, 201.

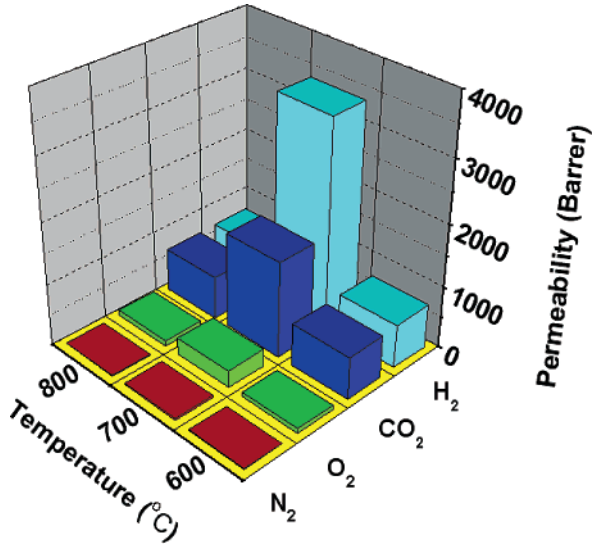

Figure 5. Gas permeability vs pyrolysis temperature for carbon/zeolite composite membranes derived from PIZ1.

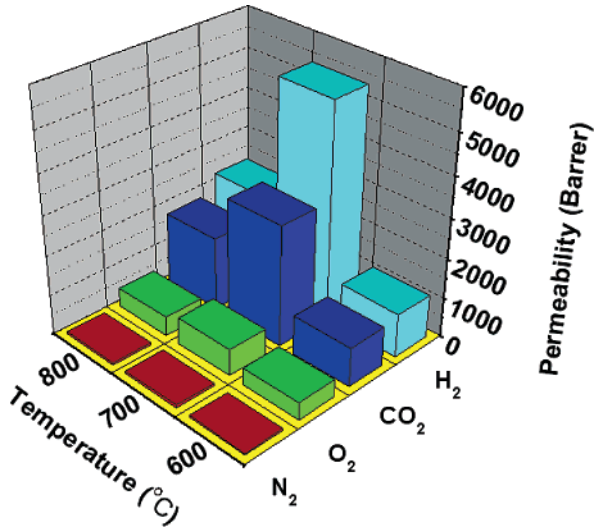

Figure 6. Gas permeability vs pyrolysis temperature for carbon/zeolite composite membranes derived from PIZ2.

The final pyrolysis temperature is another significant factor affecting the gas separation performance for the composite membranes. As shown in Figures 5−7, all gas permeabilities increase with increasing pyrolysis temperature up to 700 °C. However, the carbon/zeolite membranes pyrolyzed at 800 °C are less permeable than those pyrolyzed at 700 °C. Thus, the gas permeability through the carbon/zeolite membranes reaches a maximum value at 700 °C. In the case of the carbon/zeolite membrane derived from PIZ3, the pyrolysis of the composite precursor at 800 °C (PIZ3-800) leads to hydrogen and oxygen permeabilities of only 2932 and 523 Barrer, respectively, in comparison with 16 309 and 2146 Barrer for pyrolysis at 700 °C (PIZ2-700). The variation with pyrolysis temperature could have been affected by two parameters that determine the performance of composite membranes: (1) a change of the zeolite structure and (2) the compactness of the turbostratic carbon structure. ZSM-5 is a thermally stable zeolite, and its structure is well-kept, as seen from the XRD (Figure 3D) and TEM (Figure 4) results. Thus, the compactness of the turbostratic carbon

Table 2. Gas Permeabilities and Permselectivities Measured for the Carbon/Zeolite Composite Membranes at 25 °C

pyrolysis temp (°C)	samples	permeability (Barrer)[a]				selectivity		
		H_2	CO_2	O_2	N_2	H_2/N_2	CO_2/N_2	O_2/N_2
600	PIZ0-600	49.5	19.7	2.21	0.16	309	123	13.8
	PIZ1-600	702	680	70	5.85	120	116	12
	PIZ2-600	1078	984	431	30	36	33	14.4
	PIZ3-600	1351	1262	499	39.6	34	32	12.6
700	PIZ0-700	253	158	12	0.81	312	195	14.8
	PIZ1-700	3384	1548	275	25	135	62	11
	PIZ2-700	5399	3020	671	59	92	51	11.4
	PIZ3-700	16309	11501	2146	246	66	47	8.7
800	PIZ0-800	108	75	5.12	0.32	338	234	16
	PIZ1-800	707	690	90	9	79	77	10
	PIZ2-800	2283	1820	482	43	53	42	11.2
	PIZ3-800	2932	2581	523	66	44	39	7.9

[a] 1 Barrer = 1×10^{-10} cm^3 (STP) cm/cm^2 s cmHg.

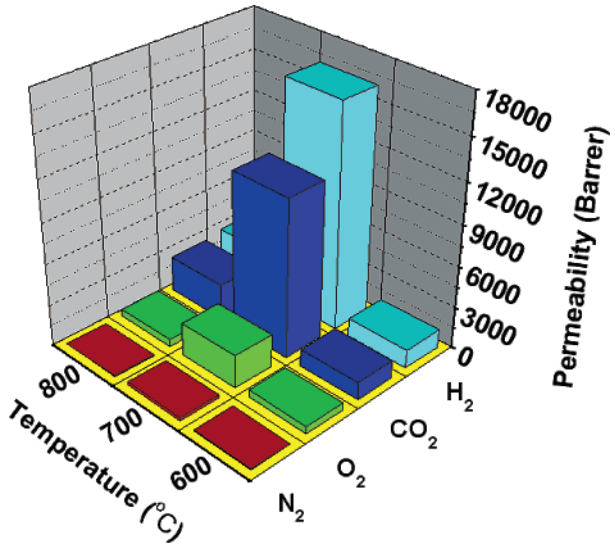

Figure 7. Gas permeability vs pyrolysis temperature for carbon/zeolite composite membranes derived from PIZ3.

structure might be the main reason for the decrease in permeability. That is, composite membranes pyrolyzed at high temperature produce a compact porous carbon morphology, which increases the diffusion resistance of the gas molecules and reduces the gas permeability. A similar densification behavior was seen in a previous study on the production of vitreous carbon by pyrolyzing phenolic resin,[21] poly(furfuryl alcohol), and poly(phenylene oxide).[22]

The permeabilities of all the selected gases measured are in the order $H_2 > CO_2 > O_2 > N_2$, which is exactly in accordance with the order of their kinetic gas diameter (Figure 8). Generally, the transport mechanism through traditional microporous membranes such as carbon membranes and silica membranes is based on a molecular sieving mechanism.[23] According to this mechanism, the separation is caused by the passage of smaller molecules of a gas mixture through the pores while the larger molecules are obstructed. Hence, the permeability of small gases through these membranes is in agreement with the order of the kinetic gas diameters. In this view, the predominant gas transport mechanism through carbon/zeolite membranes could be the molecular sieving mechanism.

The permeability and the selectivity to nitrogen of all the samples are summarized in Table 2. The H_2/N_2 selectivity and CO_2/N_2 selectivity decrease with increasing zeolite loading. The O_2/N_2 selectivity also decreases at the PIZ3 series membrane (Figure 9). However, the variety of O_2/N_2 selectivity is not obvious in the PIZ1 and PIZ2 series membranes. It is well-known that ZSM-5 shows nonselec-

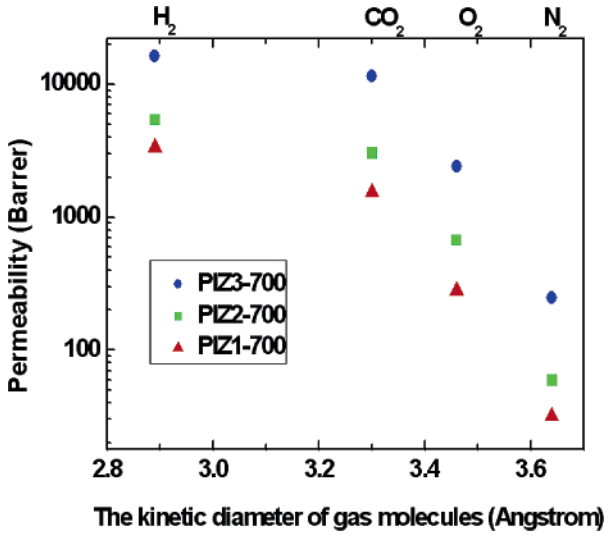

Figure 8. Gas permeability vs the kinetic diameters of gas molecules.

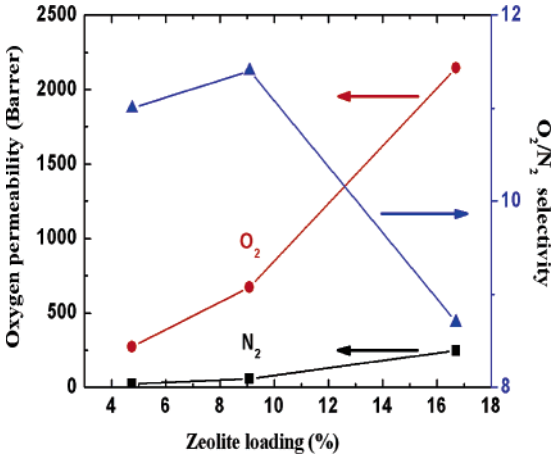

Figure 9. O_2 permeability and O_2/N_2 selectivity of composite membranes prepared at 700 °C vs zeolite loading.

(21) Pierson, H. O. *Handbook of Carbon, Graphite, Diamond, and Fullerenes: Properties, Processing, and Applications*; Noyes Publications: Park Ridge, NJ, 1993; p 126.
(22) Fitzer, E.; Schäfer, W. *Carbon* **1970**, *8*, 353.
(23) Ismail, A. F.; David, L. I. B. *J. Membr. Sci.* **2001**, *193*, 1.

tivity to oxygen and nitrogen since its pore size is larger than oxygen (3.46 Å) and nitrogen (3.64 Å). Thus, the selectivity of oxygen to nitrogen should be mainly due to the carbon matrix in the composite membranes. It is possible that the pore windows of ZSM-5 might be modified by carbon formed during the pyrolysis process, which also helps to improve the selectivity of the composite membranes.

Conclusions

Carbon/zeolite nanocomposite membranes with excellent gas separation performance were rationally designed and prepared by incorporating microporous nanosized zeolite ZSM-5 into a carbon matrix. SEM and TEM images of the as-synthesized membranes suggested that the composite membranes were defect-free and that the microstructure of the zeolite embedded in the carbon phase was not destroyed. A gas permeation test using small penetrant molecules revealed that the gas permeability was improved with increasing zeolite loading. It is believed that the dramatic increases in gas permeability resulted from abundant microchannels brought by zeolite ZSM-5 in the composite membranes. Zeolite ZSM-5 offered a favorable effect on increasing gas permeability by decreasing the gas diffusion resistance. The final pyrolysis temperature was found to have a very significant effect on the resulting separation properties of the carbon/zeolite composite membranes, and samples prepared at 700 °C showed the best gas separation performance. Therefore, manipulation of the preparation parameters (zeolite loading and final pyrolysis temperature) could tailor the desired permeability and selectivity of the membrane material. A comparison of data from single-gas and mixed-gas permeation experiments will be reported in the near future. We are convinced that the novel membrane material presented here has great potential for application in gas separation.

Acknowledgment. The support from the National Natural Science Foundation of China (No. 20276008), the DLUT-DICP joint program, the National Basic Research Program of China (G2003CB615806), and the Program for New Century Excellent Talents in Universities of China (No. NCET-04-0274) is gratefully acknowledged. Dr. T. J. Sun is acknowledged for assistance in TEM analysis and Prof. J. H. Xiu is thanked for XRD measurements.

CM061807E